





TECH BRIEFS

NATIONAL AERONAUTICS AND SPACE ADMINISTRATION

-  **Technology Focus**
-  **Electronics/Computers**
-  **Software**
-  **Materials**
-  **Mechanics/Machinery**
-  **Manufacturing**
-  **Bio-Medical**
-  **Physical Sciences**
-  **Information Sciences**
-  **Books and Reports**

INTRODUCTION

Tech Briefs are short announcements of innovations originating from research and development activities of the National Aeronautics and Space Administration. They emphasize information considered likely to be transferable across industrial, regional, or disciplinary lines and are issued to encourage commercial application.

Additional Information on NASA Tech Briefs and TSPs

Additional information announced herein may be obtained from the NASA Technical Reports Server: <http://ntrs.nasa.gov>.

Please reference the control numbers appearing at the end of each Tech Brief. Information on NASA's Innovative Partnerships Program (IPP), its documents, and services is available on the World Wide Web at <http://www.ipp.nasa.gov>.

Innovative Partnerships Offices are located at NASA field centers to provide technology-transfer access to industrial users. Inquiries can be made by contacting NASA field centers listed below.

NASA Field Centers and Program Offices

Ames Research Center

David Morse
(650) 604-4724
david.r.morse@nasa.gov

Dryden Flight Research Center

Ron Young
(661) 276-3741
ronald.m.young@nasa.gov

Glenn Research Center

Kimberly A. Dalgleish-Miller
(216) 433-8047
kimberly.a.dalgleish@nasa.gov

Goddard Space Flight Center

Nona Cheeks
(301) 286-5810
nona.k.cheeks@nasa.gov

Jet Propulsion Laboratory

Dan Broderick
(818) 354-1314
daniel.f.broderick@jpl.nasa.gov

Johnson Space Center

John E. James
(281) 483-3809
john.e.james@nasa.gov

Kennedy Space Center

David R. Makufka
(321) 867-6227
david.r.makufka@nasa.gov

Langley Research Center

Michelle Ferebee
(757) 864-5617
michelle.t.ferebee@nasa.gov

Marshall Space Flight Center

Terry L. Taylor
(256) 544-5916
terry.taylor@nasa.gov

Stennis Space Center

Ramona Travis
(228) 688-3832
ramona.e.travis@ssc.nasa.gov

NASA Headquarters

Daniel Lockney,
Technology Transfer Program Executive
(202) 358-2037
daniel.p.lockney@nasa.gov

Small Business Innovation Research (SBIR) & Small Business Technology Transfer (STTR) Programs

Rich Leshner, Program Executive
(202) 358-4920
rleshner@nasa.gov



TECH BRIEFS

NATIONAL AERONAUTICS AND SPACE ADMINISTRATION

5 Technology Focus: Test & Measurement

- 5 Test Waveform Applications for JPL STRS Operating Environment
- 5 Pneumatic Proboscis Heat-Flow Probe
- 6 Method to Measure Total Noise Temperature of a Wireless Receiver During Operation
- 6 Cursor Control Device Test Battery
- 7 Functional Near-Infrared Spectroscopy Signals Measure Neuronal Activity in the Cortex
- 7 ESD Test Apparatus for Soldering Irons
- 8 FPGA-Based X-Ray Detection and Measurement for an X-Ray Polarimeter
- 8 Sequential Probability Ratio Test for Spacecraft Collision Avoidance Maneuver Decisions

9 Manufacturing & Prototyping

- 9 Silicon/Carbon Nanotube Photocathode for Splitting Water
- 9 Advanced Materials and Fabrication Techniques for the Orion Attitude Control Motor

11 Electronics/Computers

- 11 Flight Hardware Packaging Design for Stringent EMC Radiated Emission Requirements
- 12 RF Reference Switch for Spaceflight Radiometer Calibration
- 12 An Offload NIC for NASA, NLR, and Grid Computing

15 Materials & Coatings

- 15 Multi-scale CNT-Based Reinforcing Polymer Matrix Composites for Lightweight Structures
- 15 Ceramic Adhesive and Methods for On-Orbit Repair of Re-Entry Vehicles
- 16 Self-Healing Nanocomposites for Reusable Composite Cryotanks

- 17 Pt-Ni and Pt-Co Catalyst Synthesis Route for Fuel Cell Applications

- 17 Aerogel-Based Multilayer Insulation With Micrometeoroid Protection

- 18 Manufacturing of Nanocomposite Carbon Fibers and Composite Cylinders

19 Mechanics/Machinery

- 19 Optimized Radiator Geometries for Hot Lunar Thermal Environments
- 19 A Mission Concept: Re-Entry Hopper-Aero-Space-Craft System on-Mars (REARM-Mars)

21 Physical Sciences

- 21 New Class of Flow Batteries for Terrestrial and Aerospace Energy Storage Applications
- 22 Reliability of CCGA 1152 and CCGA 1272 Interconnect Packages for Extreme Thermal Environments
- 22 Using a Blender to Assess the Microbial Density of Encapsulated Organisms

25 Information Technology

- 25 Mixed Integer Programming and Heuristic Scheduling for Space Communication
- 25 Video Altimeter and Obstruction Detector for an Aircraft
- 25 Control Software for Piezo Stepping Actuators
- 26 Optimization of Turbine Blade Dovetail Geometry

29 Software

- 29 Galactic Cosmic Ray Event-Based Risk Model (GERM) Code
- 29 Sasquatch Footprint Tool
- 29 Multi-User Space Link Extension (SLE) System

This document was prepared under the sponsorship of the National Aeronautics and Space Administration. Neither the United States Government nor any person acting on behalf of the United States Government assumes any liability resulting from the use of the information contained in this document, or warrants that such use will be free from privately owned rights.



Test Waveform Applications for JPL STRS Operating Environment

NASA's Jet Propulsion Laboratory, Pasadena, California

This software demonstrates use of the JPL Space Telecommunications Radio System (STRS) Operating Environment (OE), tests APIs (application programming interfaces) presented by JPL STRS OE, and allows for basic testing of the underlying hardware platform. This software uses the JPL STRS Operating Environment ["JPL Space Telecommunications Radio System Operating Environment," (NPO-4776) *NASA Tech Briefs*, commercial edition, Vol. 37, No. 1 (January 2013), p. 47] to interact with the JPL-SDR Software Defined Radio developed for the CoNNeCT (COmmunications, Navigation, and Networking rEconfigurable Testbed) Project as part of the SCan Testbed installed on the

International Space Station (ISS). These are the first applications that are compliant with the new NASA STRS Architecture Standard.

Several example waveform applications are provided to demonstrate use of the JPL STRS OE for the JPL-SDR platform used for the CoNNeCT Project. The waveforms provide a simple digitizer and playback capability for the S-Band RF slice, and a simple digitizer for the GPS slice ["CoNNeCT Global Positioning System RF Module," (NPO-47764) *NASA Tech Briefs*, commercial edition, Vol. 36, No. 3 (March 2012), p. 36]. These waveforms may be used for hardware test, as well as for on-orbit or laboratory checkout.

Additional example waveforms implement SpaceWire and timer modules, which can be used for time transfer and demonstration of communication between the two Xilinx FPGAs in the JPL-SDR. The waveforms are also compatible with ground-based use of the JPL STRS OE on radio breadboards and Linux.

This work was done by James P. Lux, Kenneth J. Peters, Gregory H. Taylor, Minh Lang, Ryan A. Stern, and Courtney B. Duncan of Caltech for NASA's Jet Propulsion Laboratory. Further information is contained in a TSP (see page 1).

This software is available for commercial licensing. Please contact Dan Broderick at Daniel.F.Broderick@jpl.nasa.gov. Refer to NPO-48028.

Pneumatic Proboscis Heat-Flow Probe

Applications include measuring heat flow in areas on Earth where optimal thermal isolation of heaters/temperature sensors is of paramount importance.

Marshall Space Flight Center, Alabama

Heat flow is a fundamental property of a planet, and provides significant constraints on the abundance of radiogenic isotopes, the thermal evolution and differentiation history, and the mechanical properties of the lithosphere. Heat-flow measurements are also essential in achieving at least four of the goals set out by the National Research Council for future lunar exploration. The heat-flow probe therefore directly addresses the goal of the Lunar Geophysical Network, which is to understand the interior structure and composition of the Moon.

A key challenge for heat flow measurement is to install thermal sensors to the depths ≈ 3 m that are not influenced by the diurnal, annual, and longer-term fluctuations of the surface thermal environment. In addition, once deployed, the heat flow probe should cause little disturbance to the thermal regime of the surrounding regolith.

A heat-flow probe system was developed that has two novel features: (1) it

utilizes a pneumatic (gas) approach, excavates a hole by lofting the lunar soil out of the hole, and (2) deploys the heat flow probe, which utilizes a coiled up tape as a thermal probe to reach >3 -meter depth.

The system is a game-changer for small lunar landers as it exhibits extremely low mass, volume, and simple deployment. The pneumatic system takes advantage of the helium gas used for pressurizing liquid propellant of the lander. Nor-



The Next-Generation Heat Flow Probe Concept. At left, the conceptual design of the heat flow probe mounted on the spacecraft landing system; at right, deployment of the heat flow probe.

mally, helium is vented once the lander is on the surface, but it can be utilized for powering pneumatic systems. Should sufficient helium not be available, a simple gas delivery system may be taken specifically for the heat flow probe. Either way,

the pneumatic heat flow probe system would be much lighter than other systems that entirely rely on the electrical power of the lander.

This work was done by Kris Zacny, Magnus Hedlund, Eric Mumm, Jeffrey Shasho, Philip

Chu, and Nishant Kumar of Honeybee Robotics Ltd. for Marshall Space Flight Center. For more information, contact Sammy Nabors, MSFC Commercialization Assistance Lead, at sammy.a.nabors@nasa.gov. Refer to MFS-32935-1.

Method to Measure Total Noise Temperature of a Wireless Receiver During Operation

NASA's Jet Propulsion Laboratory, Pasadena, California

A method has been developed to measure the total effective noise power in a GPS receiver, including contributions from the system temperature, the antenna temperature, interference, lossy components, etc. A known level of noise is periodically injected before the preamplifier during normal tracking, with a switch set to a very low duty cycle, so that there is insignificant signal loss for the GPS signals being tracked. Alternately, a signal of known power may be injected.

The coupling port is fed with a switch that can be controlled from the receiver's digital processing section. The switch can connect the coupling port to

a noise or signal source at a known power level. The combined system noise is measured, and nearly continuous noise calibrations are made. The effect from injected noise/signals on the performance of the GPS receiver can be less than 0.01 dB of SNR loss. Minimal additional components are required. The GPS receiver is used to measure the SNRs required to solve for the noise level. Because this measurement is referenced to the preamplifier input, it is insensitive to variations in the receiver gain.

This work was done by Lawrence E. Young, Stephan Esterhuizen, and Dmitry Turbiner of

Caltech for NASA's Jet Propulsion Laboratory. Further information is contained in a TSP (see page 1).

In accordance with Public Law 96-517, the contractor has elected to retain title to this invention. Inquiries concerning rights for its commercial use should be addressed to:

*Innovative Technology Assets Management
JPL*

Mail Stop 321-123

4800 Oak Grove Drive

Pasadena, CA 91109-8099

E-mail: iaoffice@jpl.nasa.gov

Refer to NPO-47818, volume and number of this NASA Tech Briefs issue, and the page number.

Cursor Control Device Test Battery

A suite of software-based tasks can be used for the study of cursor control devices, gloved operations, and fine motor control.

Lyndon B. Johnson Space Center, Houston, Texas

The test battery was developed to provide a standard procedure for cursor control device evaluation. The software was built in Visual Basic and consists of nine tasks and a main menu that integrates the set-up of the tasks. The tasks can be used individually, or in a series defined in the main menu.

Task 1, the Unidirectional Pointing Task, tests the speed and accuracy of clicking on targets. Two rectangles with an adjustable width and adjustable center-to-center distance are presented. The task is to click back and forth between the two rectangles. Clicks outside of the rectangles are recorded as errors.

Task 2, Multidirectional Pointing Task, measures speed and accuracy of clicking on targets approached from different angles. Twenty-five numbered squares of adjustable width are arranged around an adjustable diameter circle. The task is to point and click on the

numbered squares (placed on opposite sides of the circle) in consecutive order. Clicks outside of the squares are recorded as errors.

Task 3, Unidirectional (horizontal) Dragging Task, is similar to dragging a file into a folder on a computer desktop. Task 3 requires dragging a square of adjustable width from one rectangle and dropping it into another. The width of each rectangle is adjustable, as well as the distance between the two rectangles. Dropping the square outside of the rectangles is recorded as an error.

Task 4, Unidirectional Path Following, is similar to Task 3. The task is to drag a square through a tunnel consisting of two lines. The size of the square and the width of the tunnel are adjustable. If the square touches any of the lines, it is counted as an error and the task is restarted.

Task 5, Text Selection, involves clicking on a Start button, and then moving

directly to the underlined portion of the displayed text and highlighting it. The pointing distance to the text is adjustable, as well as the to-be-selected font size and the underlined character length. If the selection does not include all of the underlined characters, or includes non-underlined characters, it is recorded as an error.

Task 6, Multi-size and Multi-distance Pointing, presents the participant with 24 consecutively numbered buttons of different sizes (63 to 163 pixels), and at different distances (60 to 80 pixels) from the Start button. The task is to click on the Start button, and then move directly to, and click on, each numbered target button in consecutive order. Clicks outside of the target area are errors.

Task 7, Standard Interface Elements Task, involves interacting with standard interface elements as instructed in written procedures, including: drop-down

menus, sliders, text boxes, radio buttons, and check boxes. Task completion time is recorded.

In Task 8, a circular track is presented with a disc in it at the top. Track width and disc size are adjustable. The task is to move the disc with circular motion

within the path without touching the boundaries of the track. Time and errors are recorded.

Task 9 is a discrete task that allows evaluation of discrete cursor control devices that tab from target to target, such as a castle switch. The task is to follow a

predefined path and to click on the yellow targets along the path.

This work was done by Kritina Holden, Aniko Sandor, John Pace, and Shelby Thompson of Lockheed Martin for Johnson Space Center. Further information is contained in a TSP (see page 1). MSC-25214-1

Functional Near-Infrared Spectroscopy Signals Measure Neuronal Activity in the Cortex

This non-invasive monitoring method can be used to evaluate the mental state of people performing critical tasks.

John H. Glenn Research Center, Cleveland, Ohio

Functional near infrared spectroscopy (fNIRS) is an emerging optical neuroimaging technology that indirectly measures neuronal activity in the cortex via neurovascular coupling. It quantifies hemoglobin concentration ([Hb]) and thus measures the same hemodynamic response as functional magnetic resonance imaging (fMRI), but is portable, non-confining, relatively inexpensive, and is appropriate for long-duration monitoring and use at the bedside. Like fMRI, it is noninvasive and safe for repeated measurements. Patterns of [Hb] changes are used to classify cognitive state. Thus, fNIRS technology offers much potential for application in operational contexts. For instance, the use of fNIRS to detect the mental state of commercial aircraft operators in near real time could allow intelligent flight decks of the future to optimally support human performance in the interest of safety by responding to hazardous mental states of the operator. However, many

opportunities remain for improving robustness and reliability. It is desirable to reduce the impact of motion and poor optical coupling of probes to the skin. Such artifacts degrade signal quality and thus cognitive state classification accuracy. Field application calls for further development of algorithms and filters for the automation of bad channel detection and dynamic artifact removal.

This work introduces a novel adaptive filter method for automated real-time fNIRS signal quality detection and improvement. The output signal (after filtering) will have had contributions from motion and poor coupling reduced or removed, thus leaving a signal more indicative of changes due to hemodynamic brain activations of interest. Cognitive state classifications based on these signals reflect brain activity more reliably. The filter has been tested successfully with both synthetic and real human subject data, and requires no auxiliary measurement.

This method could be implemented as a real-time filtering option or bad channel rejection feature of software used with frequency domain fNIRS instruments for signal acquisition and processing. Use of this method could improve the reliability of any operational or real-world application of fNIRS in which motion is an inherent part of the functional task of interest. Other optical diagnostic techniques (e.g., for NIR medical diagnosis) also may benefit from the reduction of probe motion artifact during any use in which motion avoidance would be impractical or limit usability.

This work was done by Angela Harnivel and Tristan Hearn of Glenn Research Center. Further information is contained in a TSP (see page 1).

Inquiries concerning rights for the commercial use of this invention should be addressed to NASA Glenn Research Center, Innovative Partnerships Office, Attn: Steven Fedor, Mail Stop 4-8, 21000 Brookpark Road, Cleveland, Ohio 44135. Refer to LEW-18952-1.

ESD Test Apparatus for Soldering Irons

Prior lengthy testing now takes less than a minute.

Goddard Space Flight Center, Greenbelt, Maryland

ESDA (Electrostatic Discharge Association) ESD STM 13.1-2000 requires frequent testing of the voltage leakage from the tip of a soldering iron and the resistance from the tip of the soldering iron to the common point ground. Without this test apparatus, the process is time-consuming and requires several wires, alligator clips, or test probes, as well as additional equipment. Soldering iron tips must be tested for electrostatic

discharge risks frequently, and this typically takes a lot of time in setup and testing. This device enables the operator to execute the full test in one minute or less.

This innovation is a simple apparatus that plugs into a digital multimeter (DMM) and the Common Point Ground (CPG) reference. It enables the user to perform two of the electrostatic discharge tests required in ESD STM 13.1-2000.

The device consists of a small black box with two prongs sticking out of one end, two inputs on the opposite end (one of the inputs is used to connect the reference CPG to the DMM), and a metal tab on one side. Inside the box are wires, several washers of various materials, and assembly hardware (nuts and screws/bolts). The device is a passive electronic component that is plugged into a DMM. The operator sets

the DMM to read voltage. The operator places the heated tip of the soldering iron onto the metal tab with a small amount of solder to ensure a complete connection. The voltage is read and recorded. The operator switches the DMM to read resistance. The operator places the heated tip of the soldering iron onto the metal tab with a small amount of solder to ensure a complete

connection. The resistance is recorded. If the recorded voltage and resistance are below a number stated in ESDA ESD STM 13.1-2000, the test is considered to pass.

The device includes all the necessary wiring internal to its body so the operator does not need to do any independent wiring, except for grounding. It uses a stack of high-thermal-resistance wash-

ers to minimize the heat transfer from the soldering iron to the wiring used to measure the resistance and voltages. This minimizes thermal error.

The device allows very rapid execution of a test that is performed frequently.

This work was done by José Sancho and Robert Esser of Goddard Space Flight Center. Further information is contained in a TSP (see page 1). GSC-16611-1

FPGA-Based X-Ray Detection and Measurement for an X-Ray Polarimeter

Goddard Space Flight Center, Greenbelt, Maryland

This technology enables detection and measurement of x-rays in an x-ray polarimeter using a field-programmable gate array (FPGA). The technology was developed for the Gravitational and Extreme Magnetism Small Explorer (GEMS) mission. It performs precision energy and timing measurements, as well as rejection of non-x-ray events. It enables the GEMS polarimeter to detect precisely when an event has taken place so that additional measurements can be made. The technology also enables this function to be performed in an FPGA using limited resources so that mass and power can be minimized while reliability for a space application is maximized and precise real-time operation is achieved.

This design requires a low-noise, charge-sensitive preamplifier; a high-speed analog to digital converter (ADC); and an x-ray detector with a cathode terminal. It functions by computing a sum of differences for time-samples whose difference exceeds a programmable threshold. A state machine advances through states as a programmable number of consecutive samples exceeds or fails to exceed this threshold. The pulse height is recorded as the accumulated sum. The track length is also measured based on the time from the start to the end of accumulation. For track lengths longer than a certain length, the algorithm estimates the barycenter of charge deposit by comparing the accumulator value at the midpoint to the final accumulator value. The

design also employs a number of techniques for rejecting background events.

This innovation enables the function to be performed in space where it can operate autonomously with a rapid response time. This implementation combines advantages of computing system-based approaches with those of pure analog approaches. The result is an implementation that is highly reliable, performs in real-time, rejects background events, and consumes minimal power.

This work was done by Kyle Gregory, Joanne Hill, and Kevin Black of Goddard Space Flight Center, and Wayne Baumgartner of the University of Maryland. For further information, contact the Goddard Innovative Partnerships Office at (301) 286-5810. GSC-16367-1

Sequential Probability Ratio Test for Spacecraft Collision Avoidance Maneuver Decisions

Goddard Space Flight Center, Greenbelt, Maryland

A document discusses sequential probability ratio tests that explicitly allow decision-makers to incorporate false alarm and missed detection risks, and are potentially less sensitive to modeling errors than a procedure that relies solely on a probability of collision threshold. Recent work on constrained Kalman filtering has suggested an approach to formulating such a test for col-

lision avoidance maneuver decisions: a filter bank with two norm-inequality-constrained epoch-state extended Kalman filters. One filter models the null hypotheses that the miss distance is inside the combined hard body radius at the predicted time of closest approach, and one filter models the alternative hypothesis. The epoch-state filter developed for this method explicitly accounts

for any process noise present in the system. The method appears to work well using a realistic example based on an upcoming, highly elliptical orbit formation flying mission.

This work was done by J. Russell Carpenter and F. Landis Markley of Goddard Space Flight Center. For further information, contact the Goddard Innovative Partnerships Office at (301) 286-5810. GSC-16333-1.



Si/Carbon Nanotube Photocathode for Splitting Water

The combination of materials is expected to increase the efficiency of the redox reaction.

NASA's Jet Propulsion Laboratory, Pasadena, California

A proof-of-concept device is being developed (see figure) for hydrogen gas production based on water-splitting redox reactions facilitated by cobalt tetra-aryl porphyrins (Co[TArP]) catalysts stacked on carbon nanotubes (CNTs) that are grown on n-doped silicon substrates. The operational principle of the proposed device is based on conversion of photoelectron energy from sunlight into chemical energy, which at a later point, can be turned into electrical and mechanical power.

The proposed device will consist of a degenerately n-doped silicon substrate with Si posts covering the surface of a 4-in. (≈ 10 -cm) wafer. The substrate will absorb radiation, and electrons will move radially out of Si to CNT. Si posts are designed such that the diameters are small enough to allow considerable numbers of electrons to transport across to the CNT layer. CNTs will be grown on top of Si using conformal catalyst (Fe/Ni) deposition over a thin alumina barrier layer. Both metallic and semiconducting CNT will be used in this investigation, thus allowing for additional charge generation from CNT in the IR region. Si post top surfaces will be masked from catalyst deposition so as to prevent CNT growth on the top surface.

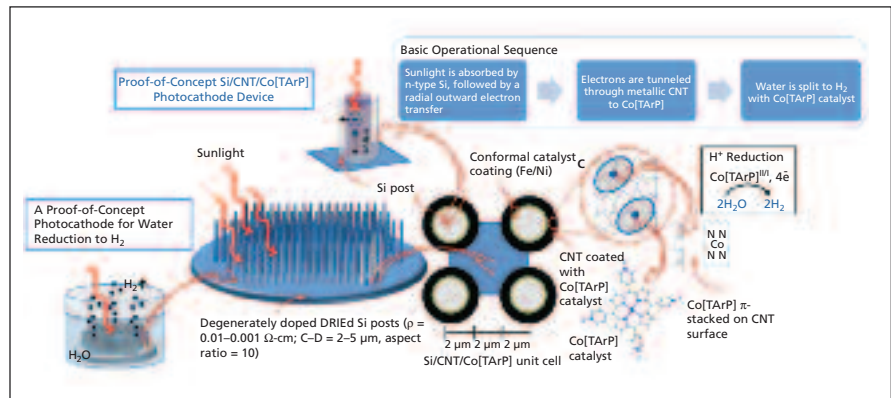


Diagram and basic operational sequence of the proof-of-concept Si/CNT/Co[TArP]. The bioinspired catalyst, Co[TArP], lowers the activation barrier for the photoactivated water splitting reaction. Rapid electron transfer from degenerately doped Si posts to metallic CNT enables the water reduction reaction. CNT material serves not only as an excellent "wire" for the electron, but as an unsurpassed substrate for the catalyst, since the mechanism (π -stacking) by which it binds Co[TArP] does not lead to significant changes in catalytic activity. The unique combination of Si, CNT and Co[TArP] is a very promising approach with a high potential to become a major breakthrough in the field of photocatalytic water splitting research and technology areas.

A typical unit cell will then consist of a Si post covered with CNT, providing enhanced surface area for the catalyst. The device will then be dipped into a solution of Co[TArP] to enable coating of CNT with Co(P). The Si/CNT/Co[TArP] assembly then will provide electrons for water splitting and hydrogen gas production. A potential of 1.23 V is needed to split water, and near ideal

band gap is approximately 1.4 eV. The combination of doped Si/CNT/Co[TArP] will enable this redox reaction to be more efficient.

This work was done by Xenia Amashukeli, Harish Manohara, Harold F. Greer, Lee J. Hall, Harry B. Gray, and Bryan Subbert of Caltech for NASA's Jet Propulsion Laboratory. For more information, contact iaoffice@jpl.nasa.gov. NPO-46951

Advanced Materials and Fabrication Techniques for the Orion Attitude Control Motor

Rhenium is ideally suited for high-temperature applications.

Marshall Space Flight Center, Alabama

Rhenium, with its high melting temperature, excellent elevated temperature properties, and lack of a ductile-to-brittle transition temperature (DBTT), is ideally suited for the hot gas components of the ACM (Attitude Control Motor), and other high-temperature applications. However, the high cost of rhenium makes fabricating these components using conventional fabrication

techniques prohibitive. Therefore, near-net-shape forming techniques were investigated for producing cost-effective rhenium and rhenium alloy components for the ACM and other propulsion applications.

During this investigation, electrochemical forming (EL-Form™) techniques were evaluated for producing the hot gas components. The investiga-

tion focused on demonstrating that EL-Form processing techniques could be used to produce the ACM flow distributor. Once the EL-Form processing techniques were established, a representative rhenium flow distributor was fabricated, and samples were harvested for material properties testing at both room and elevated temperatures. As a lower cost and lighter weight alterna-

tive to an all-rhenium component, rhenium-coated graphite and carbon-carbon were also evaluated. The rhenium-coated components were thermal-cycle tested to verify that they could withstand the expected thermal loads during service.

High-temperature electroforming is based on electrochemical deposition of compact layers of metals onto a mandrel of the desired shape. Mandrels used for electro-deposition of near-net shaped parts are generally fabricated from high-density graphite. The graphite mandrel is easily machined and does not react with the molten electrolyte. For near-net shape components, the inner surface of

the electroformed part replicates the polished graphite mandrel.

During processing, the mandrel itself becomes the cathode, and scrap or refined refractory metal is the anode. Refractory metal atoms from the anode material are ionized in the molten electrolytic solution, and are deposited onto the cathodic mandrel by electrochemical reduction. Rotation of the mandrel ensures uniform distribution of refractory material. The EL-Form process allows for manufacturing in an inert atmosphere with deposition rates from 0.0004 to 0.002 in./h (10.2 to 50.8 $\mu\text{m}/\text{h}$). Thicknesses typically range from microns to greater than 0.5 in. (13

mm). The refractory component produced is fabricated, dependably, to within one micron of the desired tolerances with no shrinkage or distortion as in other refractory metal manufacture techniques. The electroforming process has been used to produce solid, non-porous deposits of rhenium, iridium, niobium, tungsten, and their alloys.

This work was done by Sridhar Gorti and Richard Holmes of Marshall Space Flight Center, and John O'Dell, Timothy McKechnie, and Anatoliy Shchetkovskiy of Plasma Processes, Inc. For further information, contact Sammy Nabors, MSFC Commercialization Assistance Lead, at sammy.a.nabors@nasa.gov. Refer to MFS-32852-1.



Flight Hardware Packaging Design for Stringent EMC Radiated Emission Requirements

This design can be used for any electronic package that needs to meet stringent electromagnetic interference/electromagnetic compatibility (EMI/EMC) environments.

NASA's Jet Propulsion Laboratory, Pasadena, California

This packaging design approach can help heritage hardware meet a flight project's stringent EMC radiated emissions requirement. The approach requires only minor modifications to a hardware's chassis and mainly concentrates on its connector interfaces. The solution is to raise the surface area where the connector is mounted by a few millimeters using a pedestal, and then wrapping with conductive tape from the cable backshell down to the surface-mounted connector. This design approach has been applied to JPL flight project subsystems.

The EMC radiated emissions requirements for flight projects can vary from benign to mission critical. If the project's EMC requirements are stringent, the best approach to meet EMC requirements would be to design an EMC control program for the project early on and implement EMC design techniques starting with the circuit board layout. This is the ideal scenario for hardware that is built from scratch. Implementation of EMC radiated emissions mitigation techniques can mature as the design progresses, with minimal impact to the design cycle. The real challenge exists for hardware that is planned to be flown following a built-to-print approach, in which heritage hardware from a past project with a different set of requirements is expected to perform satisfactorily for a new project. With acceptance of heritage, the design would already be established (circuit board layout and components have already been pre-determined), and hence any radiated emissions mitigation techniques would only be applicable at the packaging level. The key is to take a heritage design with its known radiated emissions spectrum and repackage, or modify its chassis design so that it would have a better chance of meeting the new project's radiated emissions requirements.

This design approach addresses radiated emissions leaking mainly from connectors. Based on a history of multiple



Figure 1. This picture shows the **Design Concept**, with the pedestals and the chassis as one piece of metal. The D-sub or Micro-D connector is then mounted on the pedestal. This pedestal provides a few extra millimeters for the conductive tape to make contact with the chassis.



Figure 2. This picture shows the **Implemented Design Concept**. Conductive tape is wrapped starting with the pedestal, around the D connector, and ending at the cable backshell. This provides a continuous conductive enclosure that seals potential RF leakages from between the D connector and the chassis, and from between the cable plug and the connector receptacle.

EMC tests performed at JPL, D-connectors and micro-D connectors are known for compromising radiated emissions and causing test failures. There are two potential areas where radiated emissions can leak through: (1) the gap between the connector and the chassis (where the connector is mounted to), and (2) the gap between where the connector receptacle and the cable plug mates to. Both areas need to be shielded in order to reduce radiated emissions from leaking through these gaps. For this design, all D-connectors and micro-D connectors are mounted on an elevated surface area, known as the pedestal. The pedestal and the chassis are one piece of metal. For circuit cards that have the connector

mounted on the card, this surface pedestal may not be possible. The alternative approach would be to implement a gasket to seal the gap between the chassis and the connector. Once the cables and connectors are securely mated, conductive tape is wrapped from the backshell (metal to metal contact) of each cable all the way to the raised pedestal onto the chassis, where the connector is mounted. In this process, the tape fully encloses the backshell, connector interface, and parts of the metallic raised chassis. This effectively seals any potential radiated emissions breach coming from the connectors, including from the gap between the chassis and the connector, and from the gap between the plug and the receptacle.

The novelty of this packaging design approach is to make limited changes to heritage design and increase its chance to meet a project's stringent radiated emissions requirement. Without employing a raised surface or using a pedestal, the act of using conductive tape to seal the leakages from the connectors becomes harder, because the tape may not fully enclose the gap between the connector and the chassis. Having some elevation gives that addi-

tional surface area for the conductive tape to fully enclose the gap. The alternative to the pedestal would be to implement a gasket design as mentioned in the previous paragraph.

With this approach to packaging, D-connectors and micro-D connectors that have long been considered a weak point for radiated emissions can be improved by using conductive tape and raising the surface area of where the connector is mounted. This gives enough surface area for the tape

to fully enclose the gap between the connector and chassis, and between the cable plug and connector receptacle. This is a simple solution to reduce the impact of radiated emissions leakage from D-connectors and micro-D connectors.

This work was done by Charlene L. Lortz, Chi-Chien N. Huang, Joshua A. Ravich, and Carl N. Steiner of Caltech for NASA's Jet Propulsion Laboratory. For more information, contact iaoffice@jpl.nasa.gov. Refer to NPO-48440.

RF Reference Switch for Spaceflight Radiometer Calibration

Goddard Space Flight Center, Greenbelt, Maryland

The goal of this technology is to provide improved calibration and measurement sensitivity to the Soil Moisture Active Passive Mission (SMAP) radiometer. While RF switches have been used in the past to calibrate microwave radiometers, the switch used on SMAP employs several techniques uniquely tailored to the instrument requirements and passive remote-sensing in general to improve radiometer performance. Measurement error and sensitivity are improved by employing techniques to reduce thermal gradients within the device, reduce insertion loss during antenna observations, increase insertion loss temporal stability, and increase rejection of radar and RFI (radio-frequency interference) signals during calibration.

The two legs of the single-pole double-throw reference switch employ three

PIN diodes per leg in a parallel-shunt configuration to minimize insertion loss and increase stability while exceeding rejection requirements at 1,413 MHz. The high-speed packaged diodes are selected to minimize junction capacitance and resistance while ensuring the parallel devices have very similar I-V curves. Switch rejection is improved by adding high-impedance quarter-wave tapers before and after the diodes, along with replacing the ground via of one diode per leg with an open circuit stub. Errors due to thermal gradients in the switch are reduced by embedding the 50-ohm reference load within the switch, along with using a 0.25-in. (≈ 0.6 -cm) aluminum pre-backed substrate.

Previous spaceflight microwave radiometers did not embed the reference load and thermocouple directly within

the calibration switch. In doing so, the SMAP switch reduces error caused by thermal gradients between the load and switch. Thermal issues are further reduced by moving the custom, high-speed regulated driver circuit to a physically separate PWB (printed wiring board). Regarding RF performance, previous spaceflight reference switches have not employed high-impedance tapers to improve rejection. The use of open-circuit stubs instead of a via to provide an improved RF short is unique to this design. The stubs are easily tunable to provide high rejection at specific frequencies while maintaining very low insertion loss in-band.

This work was done by Joseph Knuble of Goddard Space Flight Center. Further information is contained in a TSP (see page 1). GSC-16398-1

An Offload NIC for NASA, NLR, and Grid Computing

New acceleration engine provides the functions of network acceleration, encryption, compression, packet-ordering, and security.

Goddard Space Flight Center, Greenbelt, Maryland

This work addresses distributed data management and access — dynamically configurable high-speed access to data distributed and shared over wide-area high-speed network environments. An offload engine NIC (network interface card) is proposed that scales at $n \times 10$ -Gbps increments through 100-Gbps full duplex. The Globus de facto standard was used in projects requiring secure, robust, high-speed bulk data transport. Novel extension mechanisms were derived that will combine

these technologies for use by GridFTP, bandwidth management resources, and host CPU (central processing unit) acceleration. The result will be wire-rate encrypted Globus grid data transactions through offload for splintering, encryption, and compression.

As the need for greater network bandwidth increases, there is an inherent need for faster CPUs. The best way to accelerate CPUs is through a network acceleration engine. Grid computing data transfers for the Globus tool set did not

have wire-rate encryption or compression. Existing technology cannot keep pace with the greater bandwidths of backplane and network connections. Present offload engines with ports to Ethernet are 32 to 40 Gbps f-d at best. The best of ultra-high-speed offload engines use expensive ASICs (application specific integrated circuits) or NPUs (network processing units). The present state of the art also includes bonding and the use of multiple NICs that are also in the planning stages for future

portability to ASICs and software to accommodate data rates at 100 Gbps.

The remaining industry solutions are for carrier-grade equipment manufacturers, with costly line cards having multiples of 10-Gbps ports, or 100-Gbps ports such as CFP modules that interface to costly ASICs and related circuitry. All of the existing solutions vary in configuration based on requirements of the host, motherboard, or carrier-grade equipment.

The purpose of the innovation is to eliminate data bottlenecks within clus-

ter, grid, and cloud computing systems, and to add several more capabilities while reducing space consumption and cost. Provisions were designed for interoperability with systems used in the NASA HEC (High-End Computing) program. The new acceleration engine consists of state-of-the-art FPGA (field-programmable gate array) core IP, C, and Verilog code; novel communication protocol; and extensions to the Globus structure. The engine provides the functions of network acceleration, encryp-

tion, compression, packet-ordering, and security added to Globus grid or for cloud data transfer. This system is scalable in $n \times 10$ -Gbps increments through 100-Gbps f-d. It can be interfaced to industry-standard system-side or network-side devices or core IP in increments of 10 GigE, scaling to provide IEEE 40/100 GigE compliance.

This work was done by James Awrach of SeaFire Micros, Inc. for Goddard Space Flight Center. Further information is contained in a TSP (see page 1). GSC-15885-1



Multi-scale CNT-Based Reinforcing Polymer Matrix Composites for Lightweight Structures

Applications include commercial aircraft, sports equipment, and automobiles.

Marshall Space Flight Center, Alabama

Reinforcing critical areas in carbon polymer matrix composites (PMCs), also known as fiber reinforced composites (FRCs), is advantageous for structural durability. Since carbon nanotubes (CNTs) have extremely high tensile strength, they can be used as a functional additive to enhance the mechanical properties of FRCs. However, CNTs are not readily dispersible in the polymer matrix, which leads to lower than theoretically predicted improvement in mechanical, thermal, and electrical properties of CNT composites. The inability to align CNTs in a polymer matrix is also a known issue. The feasibility of incorporating aligned CNTs into an FRC was demonstrated using a novel, yet commercially viable nanofiber approach, termed NRMs (nanofiber-reinforcing mats). The NRM concept of reinforcement allows for a convenient and safe means of incorporating CNTs into FRC structural components specifically where they are needed during the fabrication process.

NRMs, fabricated through a novel and scalable process, were incorporated into

FRC test panels using layup and vacuum bagging techniques, where alternating layers of the NRM and carbon prepreg were used to form the reinforced FRC structure. Control FRC test panel coupons were also fabricated in the same manner, but comprised of only carbon prepreg. The FRC coupons were machined to size and tested for flexural, tensile, and compression properties. This effort demonstrated that FRC structures can be fabricated using the NRM concept, with an increased average load at break during flexural testing versus that of the control.

The NASA applications for the developed technologies are for lightweight structures for in-space and launch vehicles. In addition, the developed technologies would find use in NASA aerospace applications such as rockets, aircraft, aircraft/spacecraft propulsion systems, and supporting facilities. The reinforcing aspect of the technology will allow for more efficient joining of fiber composite parts, thus offering additional weight savings. More robust

structures capable of withstanding micrometeoroid and space debris impacts will be possible with the enhanced mechanical properties imparted by the aligned CNTs incorporated into the fiber composite structure, as well as the potential for improved electrical and thermal properties.

The materials fabrication approach developed in the present effort is a platform for customer applications where additional reinforcement is required or would be beneficial, especially in FRC structures and component parts. Depending upon the specific customer application, the NRM could be tailored to the specific matrix resin and desired property enhancement.

This work was done by Daniel Eberly, Runqing Ou, Adam Karcz, and Ganesh Skandan of NEI Corporation, and Prof. Patrick Mather and Erika Rodriguez of Syracuse University for Marshall Space Flight Center. For more information, contact Sammy Nabors, MSFC Commercialization Assistance Lead, at sammy.a.nabors@nasa.gov. Refer to MFS-32998-1.

Ceramic Adhesive and Methods for On-Orbit Repair of Re-Entry Vehicles

Material can be applied in space to repair damage that requires heat/oxidation protection upon re-entry to Earth's atmosphere.

Lyndon B. Johnson Space Center, Houston, Texas

This adhesive is capable of repairing damaged leading edge components of re-entry vehicles while in space, and is novel with regard to its ability to be applied in the vacuum of space, and in a microgravity environment. Once applied, the adhesive provides thermal and oxidation protection to the substrate (in this case, reinforced carbon/carbon composites, RCCs) during re-entry of a space vehicle. Although there may be many formulations for repair adhesives, at the time of

this reporting, this is the first known adhesive capable of an on-orbit repair.

The adhesive is an engineered ceramic material composed of a pre-ceramic polymer and refractory powders in the form of a paste or putty that can be applied to a scratched, cracked, or fractured composite surface, covering and protecting the damaged area. The adhesive is then "cured" with a heat cycle, thereby cross-linking the polymer into a hardened material and bonding

it to the substrate. During the heat of re-entry, the material is converted to a ceramic coating that provides thermal and oxidative stability to the repaired area, thus allowing the vehicle to pass safely from space into the upper atmosphere.

Ceramic powders such as SiC, ZrB₂ and Y₂O₃ are combined with allylhydri-dopolycarbosilane (AHPCS) resin, and are mixed to form a paste adhesive. The material is then applied to the damaged area by brush, spatula, trowel, or other

means to fill cracks, gaps, and holes, or used to bond patches onto the damaged area. The material is then cured, in a vacuum, preferably at 250 °F (≈121 °C) for two hours. The re-entry heating of the vehicle at temperatures in excess of 3,000 °F (≈1,650 °C) then converts this material into a ceramic coating.

This invention has demonstrated advantages in resistance to high temperatures, as was demonstrated in more than 100 arc-jet tests in representative environments at NASA. Extensive testing verified oxidation protection for the repaired substrate (RCC), and confirmed that the microstructure of the resulting repair leads to durability and

resistance to melting or flow. Its processability and working life in a vacuum was demonstrated by NASA astronauts in glovebox processing studies, as well as on-orbit in the open space shuttle bay. All of these advantages increase the working life of NASA vehicles, as well as improve safety for any crew on a manned vehicle. The adhesive, trademarked NOAX™ or Non-Oxide Adhesive Experimental, flew on all space shuttle missions from Return To Flight (STS-114) until the final flight (STS-135) as a crack repair material for the leading edges and nose cap of the vehicle. NOAX™ was patented under U.S. Patents 7,628,878 and 7,888,277.

This work was done by James A. Riedell and Timothy E. Easter of ATK COI Ceramics, Inc. for Johnson Space Center. Further information is contained in a TSP (see page 1).

Title to this invention, covered by U.S. Patent Nos. 7,628,878 and 7,888,277, has been waived under the provisions of the National Aeronautics and Space Act (42 U.S.C. 2457 (f)). Inquiries concerning licenses for its commercial development should be addressed to:

*ATK COI Ceramics, Inc.
9617 Distribution Avenue
San Diego, California, 92121
Phone No.: (858) 621-5700*

Refer to MSC-23996-1/5218-1, volume and number of this NASA Tech Briefs issue, and the page number.

Self-Healing Nanocomposites for Reusable Composite Cryotanks

Applications for COPVs include storage of natural gas and liquid hydrogen fuel in vehicles, and marine transport of propane via tanker ships.

Marshall Space Flight Center, Alabama

Composite cryotanks, or composite overwrapped pressure vessels (COPVs), offer advantages over currently used aluminum-lithium cryotanks, particularly with respect to weight savings. Future NASA missions are expected to use COPVs in spaceflight propellant tanks to store fuels, oxidizers, and other liquids for launch and space exploration vehicles. However, reliability, reparability, and reusability of the COPVs are still being addressed, especially in cryogenic temperature applications; this has limited the adoption of COPVs in reusable vehicle designs.

The major problem with composites is the inherent brittleness of the epoxy matrix, which is prone to microcrack formation, either from exposure to cryogenic conditions or from impact from different sources. If not prevented, the microcracks increase gas permeation and leakage. Accordingly, materials innovations are needed to mitigate microcrack damage, and prevent damage in the first place, in composite cryotanks. The self-healing technology being developed is capable of healing the microcracks through the use of a novel engineered nanocomposite, where a uniquely designed nanoparticle additive is incorporated into the epoxy matrix. In particular, this results in an enhancement in the burst pressure after cryogenic cycling of the nanocomposite COPVs, relative to the control COPVs.

Incorporating a novel, self-healing, epoxy-based resin into the manufacture of COPVs allows repeatable self-healing of microcracks to be performed through the simple application of a low-temperature heat source. This permits COPVs to be repairable and reusable with a high degree of reliability, as microcracks will be remediated. The unique phase-separated morphology that was imparted during COPV manufacture allows for multiple self-healing cycles.

Unlike single-target approaches where one material property is often improved at the expense of another, robustness has been introduced to a COPV by a combination of a modified resin and nanoparticle additives. Unique nanoparticles were used that have been surface-functionalized to be compatible with the resin. Both organic and inorganic components toughen the matrix and result in a more impact-resistant COPV.

In one resin system containing an inorganic nanomaterial additive, a significant improvement in burst performance was observed after the COPV was cryo-impact-damaged and then self-healed, with a greater than 10% improvement in burst pressure after the self-healing process was performed. Initial cross-sectional analysis via microscopy showed good resin infiltration of the carbon fibers and without voids. To further enhance the capability between the nanomaterial additives and

the resin, a surface modification was successfully performed. A second specialty epoxy resin was prepared using a surface-modified nanomaterial additive, and COPVs were fabricated. Steps were taken to improve the mechanical properties of the COPVs by using a low-viscosity resin system that contained a different curing agent. This lower viscosity improves the processing of the COPV, and preliminary results show that the burst pressure of these new vessels is 20 to 25% higher than that of the original.

The self-healing concept demonstrated in this research and development effort represents a platform technology, and the self-healing property is neither restricted to the particular epoxy system used here, nor to the COPV application. Self-healing is a direct result of a unique phase separated morphology created via the resin and is aided by the nanoparticles. The self-healing function can be introduced to other customer-specific resin systems in coating, bulk, or composite applications provided that the unique phase separated morphology can be enabled in those systems.

This work was done by Daniel Eberly, Runqing Ou, Adam Karcz, and Ganesh Skandan of NEI Corporation for Marshall Space Flight Center. For more information, contact Sammy Nabors, MSFC Commercialization Assistance Lead, at sammy.a.nabors@nasa.gov. Refer to MFS-32995-1.

Pt-Ni and Pt-Co Catalyst Synthesis Route for Fuel Cell Applications

The main objective is to increase the overall efficiencies of fuel cell systems to support power for manned lunar bases.

NASA's Jet Propulsion Laboratory, Pasadena, California

Oxygen reduction reactions (ORRs) at the cathode are the rate-limiting step in fuel cell performance. The ORR is 100 times slower than the corresponding hydrogen oxidation at the anode. Speeding up the reaction at the cathode will improve fuel cell efficiency.

The cathode material is generally Pt powder painted onto a substrate (e.g., graphite paper). Recent efforts in the fuel cell area have focused on replacing Pt with Pt-X alloys (where X = Co, Ni, Zr, etc.) in order to (a) reduce cost, and (b) increase ORR rates. One of these strategies is to increase ORR rates by reducing the powder size, which would result in an increase in the surface area, thereby facilitating faster reaction rates.

In this work, a process has been developed that creates Pt-Ni or Pt-Co al-

loys that are finely divided (on the nano scale) and provide equivalent performance at lower Pt loadings. Lower Pt loadings will translate to lower cost.

Precursor salts of the metals are dissolved in water and mixed. Next, the salt mixtures are dried on a hot plate. Finally, the dried salt mixture is heat-treated in a furnace under flowing reducing gas. The catalyst powder is then used to fabricate a membrane electrode assembly (MEA) for electrochemical performance testing. The Pt-Co catalyst-based MEA showed comparable performance to an MEA fabricated using a standard Pt black fuel cell catalyst.

The main objective of this program has been to increase the overall efficien-

cies of fuel cell systems to support power for manned lunar bases. This work may also have an impact on terrestrial programs, possibly to support the effort to develop a carbon-free energy source. This catalyst can be used to fabricate high-efficiency fuel cell units that can be used in space as regenerative fuel cell systems, and terrestrially as primary fuel cells. Terrestrially, this technology will become increasingly important when transition to a hydrogen economy occurs.

This work was done by Samad A. Firdosy, Vilupanur A. Ravi, Thomas I. Valdez, and Adam Kisor of Caltech; and Sri R. Narayan of USC for NASA's Jet Propulsion Laboratory. Further information is contained in a TSP (see page 1). NPO-47885

Aerogel-Based Multilayer Insulation With Micrometeoroid Protection

The aerogel's hydrophobic nature ensures thermal performance when exposed to the environment.

Goddard Space Flight Center, Greenbelt, Maryland

Ultra-low-density, highly hydrophobic, fiber-reinforced aerogel material integrated with MLI (aluminized Mylar reflectors and B4A Dacron separators) offers a highly effective insulation package by providing unsurpassed thermal performance and significant robustness, delivering substantial MMOD protection via the addition of a novel, durable, external aerogel layer. The hydrophobic nature of the aerogel is an important property for maintaining thermal performance if the material is exposed to the environment (i.e. rain, snow, etc.) during ground installations.

The hybrid aerogel/MLI/MMOD solution affords an attractive alternative because it will perform thermally in the same range as MLI at all vacuum levels (including high vacuum), and offers significant protection from micrometeoroid damage. During this effort, the required low-density and resilient aerogel materials have been developed that are needed to opti-

mize the thermal performance for space (high vacuum) cryotank applications.

The proposed insulation/MMOD package is composed of two sections: a stack of interleaved aerogel layers and MLI intended for cryotank thermal insulation, and a 1.5- to 1-in. (≈ 2.5 - to 3.8-cm) thick aerogel layer (on top of the insulation portion) for MMOD protection. Learning that low-density aerogel cannot withstand the hypervelocity impact test conditions, the innovators decided during the course of the program to fabricate a high-density and strong material based on a cross-linked aerogel (X-aerogel; developed elsewhere by the innovators) for MMOD protection.

This system has shown a very high compressive strength that is capable of withstanding high-impact tests if a proper configuration of the MMOD aerogel layer is used. It was learned that by stacking two X-aerogel layers [1.5-in.

(≈ 3.8 -cm) thick] separated by an air gap, the system would be able to hold the threat at a speed of 5 km/s and "pass" the test. The first aerogel panel stopped the projectile from damaging the second aerogel panel. The impacted X-aerogel (the back specimen from the successful test) was further tested in comparison to another similar sample (not impacted) at Kennedy Space Center for thermal conductivity evaluation at cryogenic conditions. The specimens were tested under high vacuum and cryogenic temperatures, using Cryostat 500. The results show that the specimen did not lose a significant amount of thermal performance due to the impact test, especially at high vacuum.

This work was done by Redouane Begag and Shannon White of Aspen Aerogels, Inc. for Goddard Space Flight Center. Further information is contained in a TSP (see page 1). GSC-16440-1

Manufacturing of Nanocomposite Carbon Fibers and Composite Cylinders

Marshall Space Flight Center, Alabama

Pitch-based nanocomposite carbon fibers were prepared with various percentages of carbon nanofibers (CNFs), and the fibers were used for manufacturing composite structures. Experimental results show that these nanocomposite carbon fibers exhibit improved structural and electrical conductivity properties as compared to unreinforced carbon fibers. Composite panels fabricated from these nanocomposite carbon fibers and an epoxy sys-

tem also show the same properties transferred from the fibers.

Single-fiber testing per ASTM C1557 standard indicates that the nanocomposite carbon fiber has a tensile modulus of 110% higher, and a tensile strength 17.7% times higher, than the conventional carbon fiber manufactured from pitch. Also, the electrical resistance of the carbon fiber carbonized at 900 °C was reduced from 4.8 to 2.2 ohm/cm. The manufacturing of the

nanocomposite carbon fiber was based on an extrusion, non-solvent process. The precursor fibers were then carbonized and graphitized. The resultant fibers are continuous.

This work was done by Seng Tan and Jianguo Zhou of Write Materials Research for Marshall Space Flight Center. For more information, contact Sammy Nabors, MSFC Commercialization Assistance Lead, at sammy.a.nabors@nasa.gov. Refer to MFS-32943-1.



Optimized Radiator Geometries for Hot Lunar Thermal Environments

Lyndon B. Johnson Space Center, Houston, Texas

The optimum radiator configuration in hot lunar thermal environments is one in which the radiator is parallel to the ground and has no view to the hot lunar surface. However, typical spacecraft configurations have limited real estate available for top-mounted radiators, resulting in a desire to use the spacecraft's vertically oriented sides. Vertically oriented, flat panel radiators will have a large view factor to the lunar surface, and thus will be subjected to significant incident lunar infrared heat. Consequently, radiator fluid temperatures will need to exceed ≈ 325 K (assuming standard spacecraft radiator optical properties) in order to provide positive heat rejection at lunar noon. Such temperatures are too high for

crewed spacecraft applications in which a heat pump is to be avoided.

A recent study of vertically oriented radiator configurations subjected to lunar noon thermal environments led to the discovery of a novel radiator concept that yielded positive heat rejection at lower fluid temperatures. This radiator configuration, called the Intense Thermal Infrared Reflector (ITIR), has exhibited superior performance to all previously analyzed concepts in terms of heat rejection in the lunar noon thermal environment. A key benefit of ITIR is the absence of louvers or other moving parts and its simple geometry (no parabolic shapes). ITIR consists of a specularly reflective shielding surface and a diffuse radiating surface joined to form

a horizontally oriented V-shape (shielding surface on top). The point of intersection of these surfaces is defined by two angles, those which define the tilt of each surface with respect to the local horizontal. The optimum set of these angles is determined on a case-by-case basis. The idea assumes minimal conductive heat transfer between shielding and radiating surfaces, and a practical design would likely stack sets of these surfaces on top of one another to reduce radiator thickness.

This work was done by Dustin Ochoa of Jacobs Engineering (ESCG) for Johnson Space Center. For further information, contact the JSC Innovation Partnerships Office at (281) 483-3809. MSC-24481-1

A Mission Concept: Re-Entry Hopper-Aero-Space-Craft System on-Mars (REARM-Mars)

A reusable lander, hopper, sample-return collector cargo system (all-in-one) is proposed for Mars.

NASA's Jet Propulsion Laboratory, Pasadena, California

Future missions to Mars that would need a sophisticated lander, hopper, or rover could benefit from the REARM Architecture. The mission concept REARM Architecture is designed to provide unprecedented capabilities for future Mars exploration missions, including human exploration and possible sample-return missions, as a reusable lander, ascend/descend vehicle, refuelable hopper, multiple-location sample-return collector, laboratory, and a cargo system for assets and humans. These could all be possible by adding just a single customized Re-Entry-Hopper-Aero-Space-Craft System, called REARM-spacecraft, and a docking station at the Martian orbit, called REARM-dock. REARM could dramatically decrease the time and the expense required to launch new exploratory missions on Mars by making

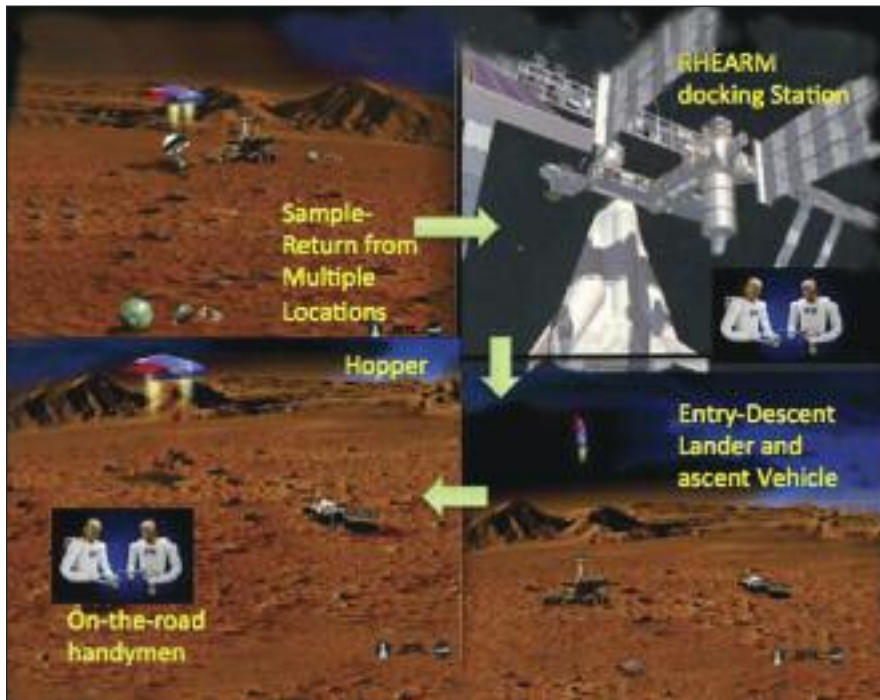
them less dependent on Earth and by reusing the assets already designed, built, and sent to Mars. REARM would introduce a new class of Mars exploration missions, which could explore much larger expanses of Mars in a much faster fashion and with much more sophisticated lab instruments.

The proposed REARM architecture consists of the following subsystems:

- **REARM-dock** that would orbit Mars could host both the spaceship traveling between Earth and the Martian orbit, as well as the REARM-spacecraft. It would repeatedly receive cargo shipped from Earth. It could also receive sample-return containers and would load them into the Earth spaceship for return to Earth. A compartment has been envisioned in the middle of the REARM-dock that would perform the exchange of cargo be-

tween the Earth spaceships and the Martian REARM-spacecraft. The cargo coming from Earth could include caches of propellant, MPEs (modular propulsion elements), batteries, spare parts for the rovers or REARM system, as well as new science payloads, which could be installed on existing rovers and sample-return containers.

- The **REARM-spacecraft** is envisioned to be a re-entry vehicle that could make round trips between the Martian orbiter and the surface of Mars using MPEs coming from the Earth, or could be solar and battery-powered similar to X37B. It would function in three different modes: (i) As a re-entry ascent/descent vehicle, cycling from the orbiter down to the surface of Mars; (ii) As a hopper, travelling (hopping) along the surface of Mars in order to relocate the rovers and other assets on



REARM is a mission concept for a multi-purpose transportation system consisting of a Martian orbiting docking station and a re-entry aero-spacecraft.

the surface using a combination of the thrusters underneath it and a stronger turbine on its back; and (iii) As a hoverer, hovering over certain areas, using the thrusters (similar to the MSL's powered descending) when positioned horizontally.

- The **sky-crane**, which is envisioned to be similar to the one used for Curiosity, could lower objects and deploy them on the surface of Mars. In addition, it could grasp objects, including samples, and pull them up.
- A **secure-attached-compartment** that is envisioned to be a part of the REARM-spacecraft could securely hold the large objects that would need to be carried by the REARM-spacecraft.

- The **sample-return container** could hold and collect the samples needed to be sent to the orbiter or to Earth. The sample-return container might be able to acquire samples directly from the surface when REARM's sky-crane would lower them to the surface.
- An **agile rover** that is envisioned to be light, fast, and small with simple science instruments such as a drill and imagers, and simple spectrometers could be used to detect and excavate important samples that would need further examination in REARM's orbital lab.
- A **scalable orbital lab** is envisioned to be a part of REARM's docking station that could be equipped with sophisticated (such as a scanner) science in-

struments by different space agencies from Earth. By extending the lab in the future, it might also be used as a safe and habitable hub for future human exploration.

- **On-the-road robotic handyman** (on-the-road Robonauts) are envisioned to perform small repairs and maintenance, such as dusting the rover's solar panels, folding the solar panels, hooking the sky-cranes securely to the rovers, changing the batteries, replacing new parts or scientific payloads, etc. They could also perform the tests and experiments inside the orbiting laboratory.

The design of the REARM-spacecraft could borrow from many existing re-entry vehicle technologies. The powered lander and sky-cranes used for MSL have already been designed, built, and tested. Also, making a docking station on the orbit of Mars could be done using previous experience of docking stations in the orbit of Earth and sending different satellites to the orbit of Mars. Therefore, the integration of the technologies needed to actually place the REARM architecture on the Martian orbit could be a conceivable endeavor.

This work was done by Faranak Davoodi of Caltech for NASA's Jet Propulsion Laboratory. For more information, contact iaoffice@jpl.nasa.gov.

In accordance with Public Law 96-517, the contractor has elected to retain title to this invention. Inquiries concerning rights for its commercial use should be addressed to:

*Innovative Technology Assets Management
JPL
Mail Stop 321-123
4800 Oak Grove Drive
Pasadena, CA 91109-8099
E-mail: iaoffice@jpl.nasa.gov
Refer to NPO-48757, volume and number of this NASA Tech Briefs issue, and the page number.*



New Class of Flow Batteries for Terrestrial and Aerospace Energy Storage Applications

Applications include energy storage in conjunction with renewable energy generation technologies such as solar, wind power, and automotive.

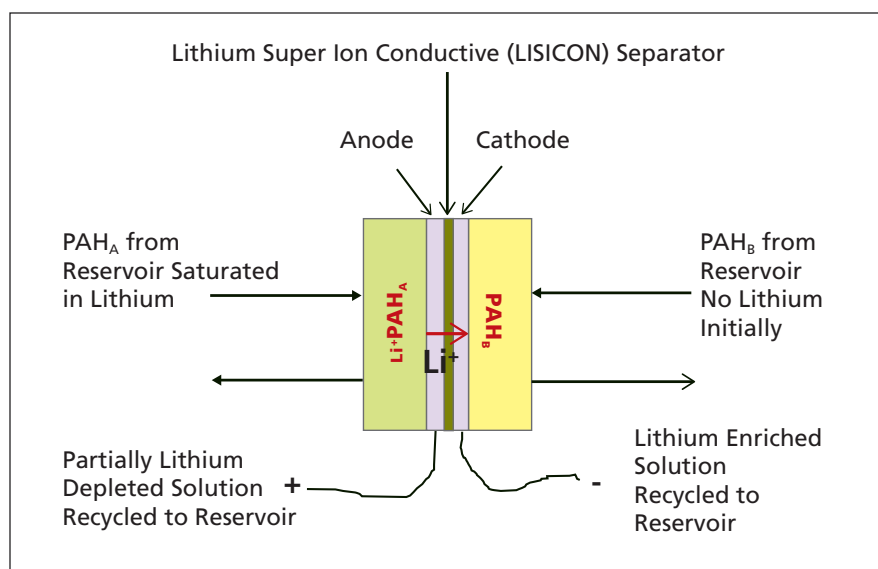
NASA's Jet Propulsion Laboratory, Pasadena, California

Future sustainable energy generation technologies such as photovoltaic and wind farms require advanced energy storage systems on a massive scale to make the alternate (green) energy options practical. The daunting requirements of such large-scale energy systems — such as long operating and cycle life, safety, and low cost — are not adequately met by state-of-the-art energy storage technologies such as vanadium flow cells, lead-acid, and zinc-bromine batteries. Much attention is being paid to redox batteries — specifically to the vanadium redox battery (VRB) — due to their simplicity, low cost, and good life characteristics compared to other related battery technologies.

NASA is currently seeking high-specific-energy and long-cycle-life rechargeable batteries in the 10-to-100-kW range to support future human exploration missions, such as planetary habitats, human rovers, etc. The flow batteries described above are excellent candidates for these applications, as well as other applications that propose to use regenerative fuel cells.

A new flow cell technology is proposed based on coupling two novel electrodes in the form of solvated electron systems (SES) between an alkali (or alkaline earth) metal and poly aromatic hydrocarbons (PAH), separated by an ionically conducting separator. The cell reaction involves the formation of such SES with a PAH of high voltage in the cathode, while the alkali (or alkaline earth metal) is reduced from such an M-PAH complex in the anode half-cell. During recharge, the reactions are reversed in both electrodes. In other words, the alkali (alkaline earth) metal ion simply shuttles from one M-PAH complex (SES) to another, which are separated by a metal-ion conducting solid or polymer electrolyte separator.

As an example, the concept was demonstrated with Li-naphthalene//Li



The **Flow Cell Technology** is based on coupling two novel electrodes in the form of Solvated Electron Systems between an alkali metal and poly aromatic hydrocarbons, separated by an ionically conducting separator.

-DDQ (DDQ is 2,3-Dichloro-5,6-dicyano-1,4-benzoquinone) separated by lithium super ion conductor, either ceramic or polymer (solid polymer or gel polymer) electrolytes. The reactants are Li-naphthalene dissolved in tetrahydrofuran (THF) with a lithium salt of 1M LiBF₄ (lithium tetra fluoroborate) in the anode compartment, and DDQ again dissolved in THF and also containing 1M LiBF₄ salt in the cathode half-cell. The solid electrolyte separator used in the first set of experiments is a ceramic solid electrolyte, available from a commercial source. The open circuit voltage of the cells is close to 3.0 V, as expected from the individual half-cell voltages of Li-naphthalene and Li-DDQ.

Upon discharge, the cell shows steady discharge voltage of -2.7 V, which confirms that the electrochemical processes do involve lithium ion shuttling from the anodic compartment to the cathode half-cell. The reversibility or rechargeability is demonstrated by charging the

partially discharged cells (i.e., with lithium present in the DDQ half). Once again, a steady voltage close to 3.0 V was observed during charge, indicating that the system is quite reversible. In the subsequent concept-demonstration studies, the ceramic electrolyte has been replaced with a gel polymer electrolyte, e.g., PVDF-HFP (poly vinylene difluoride-hexafluoropropene) gel, which has several advantages such as high ionic conductivity (almost comparable to liquid electrolyte and about 2 orders of magnitude better than the ceramic equivalent), lower cost, and possibly higher chemical stability at the anode. In addition, it can be bonded to the electrode by thermal fusion to form membrane electrode assemblies (MEAs), as is done in fuel cells.

Though the initial experiments were performed with Pt electrodes, subsequent tests with porous carbon electrodes showed better kinetics, yielding higher discharge currents. Combining

the polymer electrolytes with carbon substrates, flow-cell stacks with membrane electrode assemblies (MEAs) may be configured much like with fuel cells with suitable flow-fields in bipolar plates for an all-liquid rechargeable flow-battery.

There are several unique attributes of this flow cell, which is amongst the highest voltage flow batteries, with cell voltages higher than the prior non-aqueous 1.7 V vanadium acetylacetonate redox flow battery. (1) The reaction involves the shuttling of lithium ions from the anolyte to catholyte, much like with traditional Li-ion cells; (2) The reactions involved at both electrodes are mostly

chemical, with the oxidized or reduced lithium reacting with the liquid active materials; (3) Both the anolyte and catholyte are electronically conducting with some lithium, thus negating the need for ionic conduction through a lithium salt solution; and (4) The electrodes are only for current collection purposes, which precludes any morphological or interfacial changes at the electrode. All these features will, in principle, contribute to a long cycle life, calendar life, safety, and low self-discharge rates.

This work was done by Ratnakumar V. Bugga, William C. West, Andrew Kindler,

and Marshall C. Smart of Caltech for NASA's Jet Propulsion Laboratory. Further information is contained in a TSP (see page 1).

In accordance with Public Law 96-517, the contractor has elected to retain title to this invention. Inquiries concerning rights for its commercial use should be addressed to:

*Innovative Technology Assets Management
JPL*

Mail Stop 321-123

4800 Oak Grove Drive

Pasadena, CA 91109-8099

E-mail: iaoffice@jpl.nasa.gov

Refer to NPO-48555, volume and number of this NASA Tech Briefs issue, and the page number.

Reliability of CCGA 1152 and CCGA 1272 Interconnect Packages for Extreme Thermal Environments

CCGA packages are used in logics and microprocessor functions, telecommunications, flight avionics, and payload electronics.

NASA's Jet Propulsion Laboratory, Pasadena, California

Ceramic column grid array (CCGA) packages have been increasing in use based on their advantages of high interconnect density, very good thermal and electrical performance, and compatibility with standard surface-mount packaging assembly processes. CCGA packages are used in space applications such as in logics and microprocessor functions, telecommunications, flight avionics, and payload electronics. As these packages tend to have less solder joint strain relief than leaded packages, the reliability of CCGA packages is very important for short- and long-term space missions.

Certain planetary satellites require operations of thermally uncontrolled hardware under extremely cold and hot temperatures with large diurnal temperature change from day to night. The planetary

protection requires the hardware to be baked at +125 °C for 72 hours to kill microbugs to avoid any biological contamination, especially for sample return missions. Therefore, the present CCGA package reliability research study has encompassed the temperature range of -185 to +125 °C to cover various NASA deep space missions.

Advanced 1152 and 1272 CCGA packaging interconnects technology test hardware objects have been subjected to extreme temperature thermal cycles from -185 to +125 °C. X-ray inspections of CCGA packages have been made before thermal cycling. No anomalous behavior and process problems were observed in the x-ray images. The change in resistance of the daisy-chained CCGA interconnects was measured as a func-

tion of increasing number of thermal cycles. Electrical continuity measurements of daisy chains have shown no anomalies, even until 596 thermal cycles. Optical inspections of hardware have shown a significant fatigue for CCGA 1152 packages over CCGA 1272 packages.

No catastrophic failures have been observed yet in the results. Process qualification and assembly are required to optimize the CCGA assembly processes. Optical inspections of CCGA boards have been made after 258 and 596 thermal cycles. Corner columns have started showing significant fatigue per optical inspection results.

This work was done by Rajeshuni Ramesham of Caltech for NASA's Jet Propulsion Laboratory. Further information is contained in a TSP (see page 1). NPO-48505

Using a Blender to Assess the Microbial Density of Encapsulated Organisms

This technology has applications in medical device manufacturing to ensure device sterility.

NASA's Jet Propulsion Laboratory, Pasadena, California

There are specific NASA requirements for source-specific encapsulated microbial density for encapsulated organisms in non-metallic materials. Projects such as the Mars Science Laboratory (MSL)

that use large volumes of non-metallic materials of planetary protection concern pose a challenge to their bioburden budget. An optimized and adapted destructive hardware technology employ-

ing a commercial blender was developed to assess the embedded bioburden of thermal paint for the MSL project.

The main objective of this optimization was to blend the painted foil pieces

in the smallest sizes possible without excessive heating. The small size increased the surface area of the paint and enabled the release of the maximum number of encapsulated microbes. During a trial run, a piece of foil was placed into a blender for 10 minutes. The outside of the blender was very hot to the touch. Thus, the grinding was reduced to five 2-minute periods with 2-minute cooling periods between cycles. However, almost 20% of the foil fraction was larger (>2 mm). Thus, the largest fractions were then put into the blender and re-ground, resulting in a 71% increase in particles less than 1 mm in size, and a 76% decrease in particles greater than 2 mm in size.

Because a repeatable process had been developed, a painted sample was processed with over 80% of the particles being <2 mm. It was not perceived that the properties (i.e. weight and rubber-like nature) of the painted/foil pieces would allow for a finer size distribution. With these constraints, each section would be ground for a total of 10 minutes with five cycles of a 2-minute pulse followed by a 2-minute pause. It was observed on several occasions that a larger blade affected the recovery of seeded spores by approximately half an order of magnitude.

In the standard approach, each piece of painted foil was aseptically removed from the bag and placed onto a sterile

tray where they were sized, cut, and cleaned. Each section was then weighed and placed into a sterile Waring Laboratory Blender. Samples were processed on low speed. The ground-up samples were then transferred to a 500-mL bottle using a sterile 1-in. (\approx 2.5-cm) trim brush. To each of the bottles sterile planetary protection rinse solution was added and a modified NASA Standard Assay (NASA HBK 6022) was performed. Both vegetative and spore plates were analyzed.

This work was done by James N. Bernardini, Robert C. Koukol, Gayane A. Kazarians, Wayne W. Schubert, and Fabian Morales of Caltech for NASA's Jet Propulsion Laboratory. Further information is contained in a TSP (see page 1). NPO-48302



Σ Mixed Integer Programming and Heuristic Scheduling for Space Communication

NASA's Jet Propulsion Laboratory, Pasadena, California

Optimal planning and scheduling for a communication network was created where the nodes within the network are communicating at the highest possible rates while meeting the mission requirements and operational constraints. The planning and scheduling problem was formulated in the framework of Mixed Integer Programming (MIP) to introduce a special penalty function to convert the MIP problem into a continuous optimization problem, and to solve the constrained optimization problem using heuristic optimization.

The communication network consists of space and ground assets with the link dynamics between any two assets varying with respect to time, distance, and telecom configurations. One asset could be

communicating with another at very high data rates at one time, and at other times, communication is impossible, as the asset could be inaccessible from the network due to planetary occultation. Based on the network's geometric dynamics and link capabilities, the start time, end time, and link configuration of each view period are selected to maximize the communication efficiency within the network.

Mathematical formulations for the constrained mixed integer optimization problem were derived, and efficient analytical and numerical techniques were developed to find the optimal solution. By setting up the problem using MIP, the search space for the optimization problem is reduced significantly, thereby

speeding up the solution process. The ratio of the dimension of the traditional method over the proposed formulation is approximately an order N (single) to 2^*N (arraying), where N is the number of receiving antennas of a node. By introducing a special penalty function, the MIP problem with non-differentiable cost function and nonlinear constraints can be converted into a continuous variable problem, whose solution is possible.

This work was done by Charles H. Lee and Kar-Ming Cheung of Caltech for NASA's Jet Propulsion Laboratory. For more information, contact iaoffice@jpl.nasa.gov.

This software is available for commercial licensing. Please contact Dan Broderick at Daniel.F.Broderick@jpl.nasa.gov. Refer to NPO-48485.

Σ Video Altimeter and Obstruction Detector for an Aircraft

Lyndon B. Johnson Space Center, Houston, Texas

Video-based altimetric and obstruction-detection systems for aircraft have been partially developed. The hardware of a system of this type includes a downward-looking video camera, a video digitizer, a Global Positioning System receiver or other means of measuring the aircraft velocity relative to the ground, a gyroscope-based or other attitude-determination subsystem, and a computer running altimetric and/or obstruction-detection software.

From the digitized video data, the altimetric software computes the pixel ve-

locity in an appropriate part of the video image and the corresponding angular relative motion of the ground within the field of view of the camera. Then by use of trigonometric relationships among the aircraft velocity, the attitude of the camera, the angular relative motion, and the altitude, the software computes the altitude. The obstruction-detection software performs somewhat similar calculations as part of a larger task in which it uses the pixel-velocity data from the entire video

image to compute a depth map, which can be correlated with a terrain map, showing locations of potential obstructions. The depth map can be used as real-time hazard display and/or to update an obstruction database.

This work was done by Frank J. Delgado of Johnson Space Center and Michael F. Abernathy, Janis White, and William R. Dolson of Rapid Imaging Software, Inc. For further information, contact the JSC Innovation Partnerships Office at (281) 483-3809. MSC-24246-1/7-1

Σ Control Software for Piezo Stepping Actuators

NASA's Jet Propulsion Laboratory, Pasadena, California

A control system has been developed for the Space Interferometer Mission (SIM) piezo stepping actuator. Piezo stepping actuators are novel because they offer extreme dynamic range (cen-

timeter stroke with nanometer resolution) with power, thermal, mass, and volume advantages over existing motorized actuation technology. These advantages come with the added benefit of

greatly reduced complexity in the support electronics. The piezo stepping actuator consists of three fully redundant sets of piezoelectric transducers (PZTs), two sets of brake PZTs, and one set of

extension PZTs. These PZTs are used to grasp and move a runner attached to the optic to be moved. By proper cycling of the two brake and extension PZTs, both forward and backward moves of the runner can be achieved. Each brake can be configured for either a power-on or power-off state. For SIM, the brakes and gate of the mechanism are configured in such a manner that, at the end of the step, the actuator is in a parked or power-off state.

The control software uses asynchronous sampling of an optical encoder to monitor the position of the runner.

These samples are timed to coincide with the end of the previous move, which may consist of a variable number of steps. This sampling technique linearizes the device by avoiding input saturation of the actuator and makes latencies of the plant vanish. The software also estimates, in real time, the scale factor of the device and a disturbance caused by cycling of the brakes. These estimates are used to actively cancel the brake disturbance. The control system also includes feedback and feed-forward elements that regulate the position of the runner to a given reference

position. Convergence time for small- and medium-sized reference positions (<200 microns) to within 10 nanometers can be achieved in under 10 seconds. Convergence times for large moves (>1 millimeter) are limited by the step rate.

This work was done by Joel F. Shields of Caltech for NASA's Jet Propulsion Laboratory. For more information, contact iaoffice@jpl.nasa.gov.

The software used in this innovation is available for commercial licensing. Please contact Dan Broderick at Daniel.F.Broderick@jpl.nasa.gov. Refer to NPO-48213.



Galactic Cosmic Ray Event-Based Risk Model (GERM) Code

This software describes the transport and energy deposition of the passage of galactic cosmic rays in astronaut tissues during space travel, or heavy ion beams in patients in cancer therapy. Space radiation risk is a probability distribution, and time-dependent biological events must be accounted for physical description of space radiation transport in tissues and cells. A stochastic model can calculate the probability density directly without unverified assumptions about shape of probability density function.

The prior art of transport codes calculates the average flux and dose of particles behind spacecraft and tissue shielding. Because of the signaling times for activation and relaxation in the cell and tissue, transport code must describe temporal and microspatial density of functions to correlate DNA and oxidative damage with non-targeted effects of signals, bystander, etc. These are absolutely ignored or impossible in the prior art.

The GERM code provides scientists data interpretation of experiments; modeling of beam line, shielding of target samples, and sample holders; and estimation of basic physical and biological outputs of their experiments. For mono-energetic ion beams, basic physical and biological properties are calculated for a selected ion type, such as kinetic energy, mass, charge number, absorbed dose, or fluence. Evaluated quantities are linear energy transfer (LET), range (R), absorption and fragmentation cross-sections, and the probability of nuclear interactions after 1 or 5 cm of water equivalent material. In addition, a set of biophysical properties is evaluated, such as the Poisson distribution for a specified cellular area, cell survival curves, and DNA damage yields per cell.

Also, the GERM code calculates the radiation transport of the beam line for either a fixed number of user-specified depths or at multiple positions along the Bragg curve of the particle in a selected material.

The GERM code makes the numerical estimates of basic physical and biophysical quantities of high-energy pro-

tons and heavy ions that have been studied at the NASA Space Radiation Laboratory (NSRL) for the purpose of simulating space radiation biological effects. In the first option, properties of mono-energetic beams are treated. In the second option, the transport of beams in different materials is treated. Similar biophysical properties as in the first option are evaluated for the primary ion and its secondary particles. Additional properties related to the nuclear fragmentation of the beam are evaluated. The GERM code is a computationally efficient Monte-Carlo heavy-ion-beam model. It includes accurate models of LET, range, residual energy, and straggling, and the quantum multiple scattering fragmentation (QMSGRG) nuclear database.

This work was done by Francis A. Cucinotta of Johnson Space Center and Ianik Plante, Artem L. Ponomarev, and Myung-Hee Y. Kim of the Universities Space Research Association. Further information is contained in a TSP (see page 1). MSC-24760-1

Sasquatch Footprint Tool

The Crew Exploration Vehicle Parachute Assembly System (CPAS) is the parachute system for NASA's Orion spacecraft. The test program consists of numerous drop tests, wherein a test article rigged with parachutes is extracted or released from an aircraft. During such tests, range safety is paramount, as is the recoverability of the parachutes and test article. It is crucial to establish an aircraft release point that will ensure that the article and all items released from it will land in safe locations. A new footprint predictor tool, called Sasquatch, was created in MATLAB. This tool takes in a simulated trajectory for the test article, information about all released objects, and atmospheric wind data (simulated or actual) to calculate the trajectories of the released objects. Dispersions are applied to the landing locations of those objects, taking into account the variability of winds, aircraft release point, and object descent rate.

Sasquatch establishes a payload release point (e.g., where the payload will be extracted from the carrier aircraft) that will ensure that the payload and all objects released from it will land in a specified cleared area. The landing lo-

cations (the final points in the trajectories) are plotted on a map of the test range.

Sasquatch was originally designed for CPAS drop tests and includes extensive information about both the CPAS hardware and the primary test range used for CPAS testing. However, it can easily be adapted for more complex CPAS drop tests, other NASA projects, and commercial partners.

CPAS has developed the Sasquatch footprint tool to ensure range safety during parachute drop tests. Sasquatch is well correlated to test data and continues to ensure the safety of test personnel as well as the safe recovery of all equipment. The tool will continue to be modified based on new test data, improving predictions and providing added capability to meet the requirements of more complex testing.

This work was done by Kristin Bledsoe of Jacobs Engineering for Johnson Space Center. Further information is contained in a TSP (see page 1). MSC-25117-1

Multi-User Space Link Extension (SLE) System

The Multi-User Space (MUS) Link Extension system, a software and data system, provides Space Link Extension (SLE) users with three space data transfer services in timely, complete, and offline modes as applicable according to standards defined by the Consultative Committee for Space Data Systems (CCSDS). MUS radically reduces the schedule, cost, and risk of implementing a new SLE user system, minimizes operating costs with a "lights-out" approach to SLE, and is designed to require no sustaining engineering expense during its lifetime unless changes in the CCSDS SLE standards, combined with new provider implementations, force changes.

No software modification to MUS needs to be made to support a new mission. Any systems engineer with Linux experience can begin testing SLE user service instances with MUS starting from a personal computer (PC) within five days. For flight operators, MUS provides a familiar-looking Web page for entering SLE configuration data received from SLE. Operators can also use the Web page to back up a space mis-

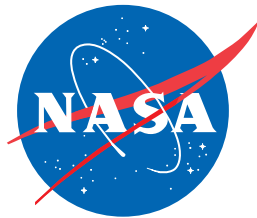
sion's entire set of up to approximately 500 SLE service instances in less than five seconds, or to restore or transfer from another system the same amount of data from a MUS backup file in about the same amount of time. Missions operate each MUS SLE service instance independently by sending it MUS "directives," which are legible, plain ASCII strings. MUS directives are usually (but not necessarily) sent through a TCP-IP (Transmission Control Protocol-Internet Protocol) socket from a MOC (Mission Operations Center) or POCC (Payload Operations Control Center) system, under scripted control, during "lights-out" spacecraft operation. MUS

permits the flight operations team to configure independently each of its data interfaces; not only commands and telemetry, but also MUS status messages to the MOC.

Interfaces can use single- or multiple-client TCP/IP server sockets, TCP/IP client sockets, temporary disk files, the system log, or standard in, standard out, or standard error as applicable. By defining MUS templates in ASCII, the flight operations team can include any MUS system variable in telemetry or command headers or footers, and/or in status messages. Data fields can be arranged within messages in different sequences, according to the mission's needs. The only con-

straints imposed are on the format of MUS directive strings, and some bare-minimum logical requirements that must be met in order for MUS to read the mission control center's spacecraft command inputs. The MUS system imposes no limits or constraints on the numbers and combinations of missions and SLE service instances that it will support simultaneously. At any time, flight operators may add, change, delete, bind, connect, or disconnect.

This work was done by Toby Perkins of Honeywell Technology Solutions Inc. for Goddard Space Flight Center. Further information is contained in a TSP (see page 1). GSC-16091-1



National Aeronautics and
Space Administration